LAWRENCE LIVERMORE LABORATORY
University of California/Livermore, California

ANTHROPOGENIC MOISTURE PRODUCTION AND ITS EFFECT ON

BOUNDARY LAYER CIRCULATIONS OVER NEW YORK CITY

Robert D. Bornstein
Yam-Tong Tam

August 1975

MASTER

ANTHROPOGENIC MOISTURE PRODUCTION AND ITS EFFECT ON

BOUNDARY LAYER CIRCULATIONS OVER NEW YORK CITY[*]

by

Robert D. Bornstein
Department of Meteorology
San Jose State University
San Jose, California 95192

and

Atmospheric & Geophysical
  Sciences Division
Lawrence Livermore Laboratory
University of California
Livermore, California 94550

and

Yam-Tong Tam
Department of Meteorology
San Jose State University
San Jose, California 95192

INTRODUCTION

Until recently, studies of the atmospheric moisture content at the surface in and around cities have shown that, on the average, cities are somewhat drier than their rural surroundings. Average relative humidities have generally been found to be several percent lower in cities than in nearby rural areas; also, absolute humidities were also found to be slightly lower in the built-up areas. The main reason given for these humidity differences was the lower evaporation rates in the city than in the country. This reduction occurs because rainfall is retained by vegetation covered rural surfaces, while rapid run-off occurs in asphalt and concrete covered cities (Peterson 1969).

Recently, Chandler (1967) obtained atmospheric moisture data from a series of automobile transverses in and around London, England during three summer nights with low wind speeds, clear skies, and well developed urban heat islands. He found that measured urban vapor pressures were higher than nearby rural vapor pressures, with the reverse true for relative humidities. He attributed the higher nighttime urban absolute humidity to the reduced amount of dew formation in urban areas and to the addition of water to the urban atmosphere from anthropogenic sources.

Similar results were found by Ackerman (1971) in an analysis of seven years of dew point data from urban Midway Airport in Chicago and from rural Argonne National Laboratory, 125 miles SW of Chicago. Results showed: 1) an urban moisture excess when all of the data were considered, 2) an urban moisture excess for the nighttime data, 3) an urban moisture deficit for the daytime data, and 4) an urban moisture excess for the winter daytime data. Thus during the times when combustion was a major

source of moisture, the urban atmosphere was more moist than the rural
atmosphere. These results are consistent with those of Auer and
Dirks (1974), who found that the air over St. Louis was drier than that
over its nearby rural areas during summer daytime periods. Urban
moisture excesses have also been found by Kopec (1973) and Goldreich
(1974), while Hage (1972) showed that anthropogenic moisture emissions
can enhance the formation of low-temperature fog in the city of Edmonton.

Vertical and horizontal moisture distributions in and around NYC
were studied by Lorenzen (1972) and Bornstein, et al. (1972) to determine
the vertical extent of urban-rural moisture differences. Sixty-two
helicopter soundings of temperature, wet-bulb depression, and pressure
height were obtained during three early morning periods and during one
late afternoon period in 1964.

Results from the analysis of the above data (fig. 1) showed that the
following values are larger at night than during the day: 1) urban heat
island values, 2) urban excesses in absolute humidity, 3) urban relative
humidity deficits below 250 m, and 4) urban relative humidity excesses
at heights between 250 and 500 m.

The data used by Bornstein, et al. (1972) were collected from 1964
to 1969 as part of a U.S. Public Health Service sponsored grant to the
late Ben Davidson of the Department of Meteorology and Oceanography at
New York University. As described by Davidson (1967), the main goal of
the project was the development of a sophisticated model for the
prediction of the distribution of SO_2 in the NYC metropolitan area
(Shieh, et al. 1969).

While the data obtained by the NYU project were used in various studies of the urban boundary layer over NYC, the original data set was never published, due to the untimely death of the project's principal investigator. In the belief that NYU/NYC data set is unique, and that it could be extremely useful to persons interested in the urban boundary layer over NYC, much of the original data has recently been published by Bornstein, et al. (1975) under a grant from the U.S. Environmental Protection Agency, and are on file with its Meteorology Laboratory at Research Triangle Park. An important component of the NYU/NYC data is an area and point source emission inventory for the production of SO_2, heat, and moisture from anthropogenic sources within the NYC metropolitan area during 1965.

The main goals of the current research reported herein are: 1) to determine the magnitude and variation in time and space of the anthropogenic moisture flux in NYC, 2) to determine the effects of the observed moisture excess on the dynamics of the urban boundary layer over NYC, and 3) to determine the fraction of the observed moisture excess over NYC that is due to each of the following: area source emissions, point source emissions, and reduced nighttime condensation rates in the urban areas, as compared to those in nearby rural areas.

The first of these goals has been carried out under a grant from the U.S. Environmental Protection Agency to the Department of Meteorology at San Jose State University, while the second part has been accomplished by use of the computer facilities at Lawrence Livermore Laboratory. The third section is currently being carried out under a grant from the National Science Foundation to the Department of Meteorology at SJSU.

In carrying out the second and third parts, the two dimensional, non-steady "URBMET" (for urban meteorology) urban boundary layer model of Bornstein (1975) has been used to predict the temporal and spatial distribution of wind, temperature, and moisture within the urban boundary layer. The surface boundary condition for the absolute humidity in these simulations is being obtained from the temporal and spatial distribution of the anthropogenic moisture production in NYC, as obtained from the fuel usage inventory compiled during the original NYU air pollution project.

ANTHROPOGENIC MOISTURE EMISSIONS

Most of the study region (fig. 2) has an elevation that is close to mean sea level, but the northwest 10% of the area consists of highlands which range in elevation from 250 to 500 feet above mean sea level. About 30% of the study area is water, while 60% is open country, and 10% has been built up for urban and suburban uses.

During the original NYU project an unpublished inventory of the annual emission of SO_2 from the known area and point sources in the New York Metropolitan region was compiled (Ingram, et al. 1965). Point source emission information were obtained through the use of questionnaires, while area source emissions from both fixed and mobile sources were computed from fuel usage data obtained from the following sources: 1) the U.S. Bureau of Mines, which publishes an annual report on the shipments of fuel oil, 2) the NY Oil Heating Association, 3) the American Petroleum Institute, 4) the NYC Council Committee on Air Pollution, 5) the NYC Housing Authority, 6) the NYC Air Pollution

Control Agency, 7) the NYC Fire Department, and 8) the NYC Licensing
Agency, which controls the installation, registration, licensing and
insurance of each furnace or power plant in NYC. The seven main types
of fuel consumed in the NYC area, the uses to which they are put, and
their annual rates of consumption are listed in table 1.

Because fossil fuels are composed of carbon, hydrogen, and sulfur, etc.,
the combustion of these fuels produces oxides of sulfur, oxides of nitrogen,
carbon monoxide, carbon dioxide, aldehydes, hydrocarbons, particulates,
and water vapor. The quantities of these products put into the atmosphere
depend on the rate of the combustion process, the content of impurities
per unit mass, the equipment used for the combustion process, and the
kinds of control devices that might have been installed. For example,
in the steam boilers of Consolidated Edison power plants, 1.4 lbs of
steam are added per 100 lbs of residual oil consumed. This is done in
order to atomize the oil, so as to increase the efficiency of the combustion
process. Thus the water vapor emission rate from these stacks is greater
than from other point sources.

The basic equation for the production of water from the combustion
of coal (after the hydrocarbons have been broken down) is

$$2H_2 + O_2 \rightarrow 2H_2O \quad , \tag{1}$$

while the general formula for the combustion of oil and gas is

$$C_xH_y + (x+\tfrac{y}{4})\, O_2 \rightarrow x\, CO_2 + \tfrac{y}{2}\, H_2O \quad , \tag{2}$$

where

$$y = 2x + 2 \tag{3}$$

if the hydrocarbon C_xH_y is saturated. Thus for coal, one gram of

hydrogen produces 18 grams of water, while y grams of H_2 per mole of gas
or oil produces 18Y/2 or 9Y grams of water per mole, where 18 is the
ratio of the molecular weights of water and hydrogen.

The water production from each component of natural gas (table 2)
was evaluated by multiplying the coefficient of the final term of Eq. (2),
i.e., Y/2, by the percentages in the middle column of the table. Water
production factors for each of the seven fuel types used in NYC are shown
in table 3, where the liquid water content of coal is determined by
drying under standard conditions for one hour at 104 to 110 C.

The five boroughs of NYC (identified by name in fig. 1) were gridded
into 1 mile by 1 mile areas, and the following equation was used to
evaluate the magnitude of the annual anthropogenic moisture production
M_A from each of the grid areas:

$$M_A' = \sum_{i=1}^{7} \frac{S_A \cdot P_i \cdot M_i}{S_i} \quad , \tag{4}$$

where the definition and units for each symbol are found in Appendix A.

Note that the product of S_A (from the unpublished SO_2 inventory of
Ingram, et al. (1965) - now published by Bornstein, et al. (1975)) and P_i
(table 4) gives the annual emission of SO_2 from the i-th fuel in a
particular grid in tons per year. Values of P_i were kept constant in each
borough because the usage of each fuel in all of the grid areas was not
available. Where the values were available, a random check showed that
the magnitudes of P_i in a given borough were within $\pm$ 5% of the mean values
used in Eq. (4). The product of S_A times P_i divided by S_i (table 5) gives
the annual usage of the i-th fuel in the particular grids while values of
M_i (table 3) include the release of gaseous and liquid moisture.

Annual area source (fixed and mobile) emissions of anthropogenic moisture in NYC in 1965 in 10^{10} gm per year (fig. 3) were obtained by the summation of the seven partial emission rates of Eq. (4). The origin of the grid used in the figure is at Battery Park, which is at the southern tip of Manhattan. The annual emission data were converted into average hourly "fluxes" (fig. 4) which have the units of 10^{-5} gm cm^{-2} hr^{-1} and which can be used as the lower (flux) boundary conditions in a numerical boundary layer model of the urban atmosphere, as is being done by Tam (1975).

Because some areas in NYC are source free (such as Central Park and the rivers around Manhattan), the "fluxes" of the previous figure were recomputed in terms of emission "intensities", i.e., the emission of H_2O per unit of production area per time. This increased the maximum emission from 2.2 x 10^{-5} gm cm^{-2} min^{-1} to 4.3 x 10^{-5} gm cm^{-2} min^{-1}. The second value corresponds to a 22.6 cm per year annual evaporation rate, which is about 25% of the annual evaporation rate in the coastal Atlantic off of NYC (Jacobs 1951).

For studies requiring a more detailed emission pattern, the above computations were repeated on 0.5 mile by 0.5 mile area source grid over Manhattan (see Bornstein, et al. 1975), the region of maximum H_2O emission. In computing the emission rates for the finer grid, the emissions from the larger grid areas were assumed to be homogeneously distributed over the built up areas of the city, while emissions from the rivers around Manhattan, and from Central Park, were taken to be zero.

Anthropogenic moisture production in NYC by borough (table 6) shows that Staten Island contributes only a very small fraction of the total area source emission in NYC (and hence it is not cross hatched in fig. 1), while Queens contributes the maximum amount of any borough. Production by fuel type (table 7) shows that residual oil produces more moisture in NYC than does any other fuel type, while production by source type (table 8) shows that domestic space heating produces a larger amount of anthropogenic moisture than any other source type.

Estimates of the hourly emission rates of anthropogenic moisture from the fixed, but not mobile, area sources in NYC were made using data obtained from timers which were attached to boilers located in selected buildings. The resulting data were used by Halpern, et al. (1971) to relate the number of minutes per day that the boilers were in operation to the degree day value D computed as follows:

$$D = 65 - \overline{T}, \qquad \overline{T} \leq 65,$$

or (5)

$$D = 0 \qquad , \qquad \overline{T} > 65,$$

where $\overline{T}$ is the average daily temperature of a given day in F.

The boiler timer data were then used by Halpern, et al. (1971) to develop the following equation which relates the daily emission rate of H_2O from a particular area source to the annual emission rate from that area source:

$$M_D = \left(\frac{0.7}{4871} D + \frac{0.3}{365} \right) M_A .$$ (6)

The above relationship shows that 30% of the annual emission of H_2O from each area source is due to the production of hot water at a uniform rate throughout the year. The remaining 70% is due to space heating,

which is dependent on the average daily temperature. Note, that the
annual sum of the daily degree day values for New York City is the 4871
appearing in the equation.

If M_A was spread uniformly over the year, then on each day 0.27% of
the total would be emitted. However, when Eq. (6) is used to pro-rate
M_A according to T (fig. 5) it is found that the value of $(M_D/M_A) \cdot 100\%$
varies linearly from 1.02% for a $\overline{T}$ of 0 F to 0.08% for a $\overline{T}$ equal to or
greater than 65 F. Thus the emission on a cold day can be as much as an
order of magnitude greater than that on a hot day.

The same boiler timer data were used by Halpern, et al. (1971) to
develop curves showing the diurnal variation in winter, when most of the
fuel is consumed for space heating, and in summer, when most of the fuel
is used for the production of hot water in the hours near sunrise and
sunset. These results were used by Leahey and Friend (1971) to compute
the spatial distribution of the annual and daily production of anthropogenic
heat in New York from area sources due to fossil fuel usage. They can be
used to produce the same information for the anthropogenic moisture flux
in NYC.

In the NYC area in 1965 there were 378 point sources of SO_2 which were
found to have an annual emission rate of at least 100 tons of SO_2. The
205 point sources within the city emitted 3.67×10^5 tons of SO_2 per year,
or about one-half of that emitted by the area sources within the city.

In general, the rate of consumption by power plants, industrial
processes, and automobiles changes only slightly throughout the year.
However, the emission rates of some industrial and commercial sources do
vary significantly over the year, and the emission rates of many point

sources do possess a diurnal variation. Where it was available, this information has been tabulated by Bornstein, et al. (1975), as has been the stack height and heat emission data needed in plume rise calculations. Thus the NYU/NYC data set contains the information needed to evaluate the area source and point source emissions of anthropogenic moisture in NYC for use as the surface flux boundary condition for moisture in an urban boundary layer model of NYC.

NUMERICAL SIMULATIONS

In the basic URBMET model, finite difference solutions to the vorticity and energy equations are obtained in a vertical plane in the direction of a constant geostropic wind. The vertical fluxes of heat and momentum are assumed to be constant with height in a lower, analytical, surface boundary layer, while they generally decrease with height in an upper, numerical finite-difference, transition layer.

The transition layer is assumed to be hydrostatic and Boussinesq, with the latter assumption implying incompressible flow. All lateral gradients are assumed to be zero, except for that of the undisturbed pressure, which corresponds to a constant geostropic wind. Adiabatic motions are also assumed, while diffusion effects in the direction of the geostropic wind are assumed to be insignificant as compared to advective effects. Initially, adiabatic lapse rates are assumed, as the heat island simulations are assumed to commence at 1800 LST. The eddy exchange coefficients used in the transition layer in URBMET are computed from a third-order-polynomial developed by O'Brien (1970). Details on the formulation of the model can be found in Bornstein (1975), hereafter refered to as B.

One modification of the original URBMET model in the current study was the inclusion of a continuity equation for water vapor, under unsaturated conditions, given by

$$\frac{\partial q'}{\partial t} = \frac{\partial (uq')}{\partial x} + \frac{\partial (wq')}{\partial z} + \frac{\partial}{\partial z} \left(K_q \frac{\partial q'}{\partial z} \right) \quad , \tag{7}$$

where K_q was taken equal to K_H. Because of this equality, the surface layer profiles for q' are identical to those for θ', if q and q_* replace θ and θ_*, respectively, in the various surface boundary layer equations in B. In addition, the potential temperature θ is replaced by the virtual potential temperature θ_v. The two are related by

$$\theta_v = [1 + 0.61 \, q]\theta \quad , \tag{8}$$

where each of the three variables, in the absence of any initial variations, can be given by the sum of a space average constant and a perturbation quality resulting from the urban induced circulations. If

$$\theta' \ll \theta_m \quad , \tag{9}$$

it can be shown that

$$\theta_v' \approx \theta' + 0.61 \, \theta_m q' \quad , \tag{10}$$

and thus θ_v' replaces θ' everywhere in the model equations given in B. The second change in URBMET was concerned with the choice of the magnitude of the time step used in integration, and this is discussed in Bornstein and Robock (1975).

An interlaced grid was used in this study, as it considers velocity components to be the average inflow and outflow rates on horizontal and vertical elements of a cube. Previous studies have discussed the superiority of variable grid spacing in achieving high resolution near the surface and

near discontinuities in surface characteristics. Accordingly, the 16 by 16 grid network used in the present study (table 9) possesses such a spacing near the surface, and in the vicinity of the city. A list of the boundary conditions on q' currently used is given below.

$$q' = a(x,t) \quad , \quad z = 0 \quad , \tag{11}$$

$$\text{continuity of } q' \text{ and } \frac{\partial q'}{\partial z} \quad , \quad z = h \quad , \tag{12}$$

$$q' = 0 \quad , \quad z = H \quad , \tag{13}$$

$$\frac{\partial (uq')}{\partial x} = 0 \quad , \quad \text{upwind boundary} \quad . \tag{14}$$

At each time step, following an initialization process described below, the following is performed: determination of the new values of θ_v' and q' at the surface; construction of the constant flux layer using the latest values of θ_v', q', and U at the surface, and at the lowest finite difference grid; and determination of the new q', θ_v', ζ, ψ, u, w, v, and U fields, respectively, using the newest available values of all parameters and done in a manor described in Bornstein and Robock (1975).

The initial conditions were considered to be those at the beginning of an urban heat island episode, i.e., at 1800 LST, and thus the following initialization procedure was carried out. First, the URBMET model was used to simulate the one-dimensional, neutral, dry planetary boundary layer over homogeneous terrain by assuming the following conditions

$$\frac{\partial}{\partial x} = w = 0 \tag{15}$$

$$\gamma = \Gamma \tag{16}$$

$$\theta_v' = 0 \tag{17}$$

$$q' = q_m = 0 \quad . \tag{18}$$

Justification of the assumption contained in Eq. (16) for the hours
near 1800 LST can be found in the observations obtained over cities
(Bornstein 1968), as well as in those from rural O'Neill (Kuo 1968).

Simulations were carried for values of the surface roughness
parameter z_0 of 1 and 3m, and for values of the geostrophic wind u_g of
3 mps. The values for z_0 were chosen to be typical of areas with buildings
of one and six stories (Lettau 1969). The simulations were carried out
using a constant value of 15 sec for the time step of integration, and
were concluded when equilibrium conditions were obtained, i.e., when the
final accelerations of the damping inertial oscillation were less than
0.1 cm $sec^{-1} hr^{-1}$.

The resulting equilibrium wind profiles were then used as the initial
conditions for simulations reproducing the two-dimensional equilibrium
distributions of wind over a rough city under conditions of neutral
stability. Thus, the conditions expressed in Eq. (15) were no longer
used, but as the results of these new simulations provided the initial
conditions for the heat island simulations discussed below, the conditions
shown in Eqs. (16) - (18) were still used.

Two-dimensional, equilibrium wind distributions for the rough city
cases were obtained after 3 hours of simulated time, using an equal
advection and diffusion time step of 15 sec. The results of these
simulations showed that the values of the total horizontal wind speed at
the urban sites at heights up to several hundred metres were reduced in
magnitude below those at corresponding heights at the upwind rural
boundary. The maximum difference in speed occurred at the first grid
point above the surface, and over the downwind half of the city. The

maximum upward and downward values of the corresponding vertical velocities were associated with the areas of maximum convergence and divergence at the upwind and downwind edges of the city, respectively. These results are presented in B.

Simulations were carried out to reproduce effects on the structure of the urban boundary layer, during the hours from 1800 to 1000 LST, resulting from higher urban than rural values of z_o and surface temperature, but not q'. Hence, the conditions expressed by Eqs. (16) and (17) were no longer used, but Eq. (18) was still applied.

The urban and rural surface cooling rates were estimated from the observations in and around urban Montreal by Oke and East (1971). These observations indicated that the rural atmosphere near the surface cooled rapidly in the evening hours before midnight, while the urban atmosphere near the surface was maintained at a nearly constant temperature during the same period. After midnight both regions cooled at about 50% of the rate found at the rural site before midnight. Therefore, the magnitude of the heat island near the surface increased with time in the early evening, and then remained constant until morning. Thus, the following surface cooling and warming rates were assumed:

Period (LST)	Urban (C hr^{-1})	Rural (C hr^{-1})
1800-2400	0.0	-1.0
2400-0600	-0.5	-0.5
0600-1000	1.0	3.0

These simulations were carried out using a variable time step for both the advective and diffusive processes (Bornstein and Robock 1975). The cooling rates prescribed above caused formation of a surface based inversion in the rural areas, and the advection of cool rural air over

the uncooled urban surface during the first six hours of the simulations caused formation of a slightly unstable layer near the urban surface. During the second six hours of simulation, the decreased surface cooling rates slowed the rate of increasing stability at rural sites, while the urban cooling was unable to completely overcome the effects of advection, and thus Richardson numbers in the city remained slightly negative.

The horizontal wind field resulting after six hours of simulated time showed a region of decreased wind speeds, as compared to those at the upwind rural boundary. This region was found upwind of, and above, a region in which speeds are higher than those at the upwind boundary. A smaller region of decreased speeds was also seen, downwind of the city near the surface. The corresponding vertical velocity field showed a region of sinking air over the city, sandwiched between two regions of upward motion. Again, results are presented in B.

The final simulations were carried out to reproduce the effects of an anthropogenic source of moisture on the structure of the urban boundary layer. Thus, the conditions expressed by Eq. (18) are no longer used; instead the background level of moisture q_m was arbitrarily set equal to 10 gm kg^{-1}. In addition, it was assumed that the surface value of q' at the urban grid points increased by 0.25 gm kg^{-1} hr^{-1}.

The excess moisture thus placed into the urban atmosphere was advected and diffused vertically and/or horizontally, as expressed by Eq. (7). A typical distribution of q' after 12 hours of simulated time at 0600 LST (fig. 6) shows the effects of the advection and diffusion.

The vertical variation of the difference between the values of the perturbation specific humidity q' over the downwind urban edge and those

at the upwind model edge at 0600 LST (the right hand half of fig. 7)
produces a buoyancy effect, as wet air is less dense than dry air. This
enhances the buoyancy produced by the urban heat island effect. At the
same height above the surface, the magnitude of the buoyancy produced by
the urban moisture excess at any point is given by the difference between
the value of $\theta_v' - \theta'$ at the upwind model boundary and that at the point
(fig. 7). From these values, and from the values of the total predicted
buoyancy, the vertical variation of the buoyancy due to the heat island
effect was computed. The results (table 10) indicate that, near the
surface, the additional buoyancy due to the moisture excess is about
10% of that due to the heat island effect.

However, observations of the moisture excess over New York City by
Bornstein, et al. (1972) indicate that the moisture excess of the
urban atmosphere in the present simulation could be increased by a
factor of two. Even with the amount of anthropogenic moisture currently
specified there is a noticeable increase in the magnitude of the urban
breeze effect (fig. 8) at the center of the urban area. The maximum
increase of ΔU in the case of an urban moisture excess (Case 2) over
those from the case of no urban moisture excess (Case 1) is about
8 cm sec^{-1}, or about 15%.

SUMMARY

A heat and moisture excess over of New York City has been shown to exist by use of helicopter soundings of temperature and wet bulb depression. For three early morning flights, the moisture excess was about 0.9 gm m^{-3}, which represented an increase of about 10% over values at nearby rural sites. The humidity and moisture excesses were generally highest over the central part of the city, and then decreased over the peripheral urban areas, implying the existence of a heat and moisture "dome" over NYC.

The magnitude of the temporal and spatial distributions of anthropogenic moisture emissions in NYC from fixed and mobile area sources were estimated using fuel usage data collected during the NYU/NYC urban air pollution dynamics project of 1964-9. The maximum annual emission rate from a particular square mile in Manhattan was found to be equal to about 25% of the annual evaporation rate in the coastal Atlantic off of NYC.

The URBMET urban boundary layer model was used to evaluate the effects on the dynamics of the urban boundary layer resulting from the buoyancy associated with an observed urban moisture excess. Results indicated that the buoyancy produced by the moisture excess was about 10% of that produced by the urban heat island effect. This excess buoyancy enhanced the strength of the "urban breeze" effect by about 15% over what had resulted due to the heat island effect alone.

Work currently in progress seeks to determine the fraction of the observed nighttime moisture excess over NYC that is due to each of the following: area source emissions of moisture, point source emissions of moisture, and reduced nighttime condensation rates in the urban areas, as compared to those in nearly rural areas. In this work, the flux of

anthropogenic moisture into the atmosphere is used as a surface boundary condition for the URBMET boundary layer model.

There is no completely satisfactory method of incorporating area and point source emissions of moisture into a boundary layer model. In previous models area sources of heat have been included in surface energy balances, even though some of this energy enters the atmosphere through the sides and tops of buildings. In addition, point sources cannot be represented in two dimensional finite difference boundary layer models, which can only treat line and area sources. Thus, work remains to be done in order to accurately represent the effects of anthropogenic heat and moisture on the structure of the urban boundary layer.

REFERENCES

Ackerman, B.
    1971. MOISTURE CONTENT OF CITY AND COUNTY.
    Preprints of the Conference on Air Pollution Meteorology.
    American Meteorological Society, 154-158.

Auer, A. H., and R. A. Dirks.
    1974. CONTRIBUTIONS TO AN URBAN METEOROLOGICAL STUDY: METROMEX.
    Bull. Amer. Meteor. Soc., 55 (2), 106-110.

Bornstein, R.D.
    1968. OBSERVATIONS OF THE URBAN HEAT ISLAND EFFECT IN NEW YORK CITY.
    J. of App. Meteor., 7 (4), 575-582.

Bornstein, R. D., A. Lorenzen, and D. Johnson.
    1972. RECENT OBSERVATIONS OF URBAN EFFECTS ON WINDS, MOISTURE, AND
    TEMPERATURE IN NEW YORK CITY.
    Preprints of the Conference on Urban Environment, Oct. 31- Nov. 2, 1972.

Bornstein, R. D.
    1975. THE TWO-DIMENSIONAL URBMET URBAN BOUNDARY LAYER MODEL.
    Accepted by the J. Appl. Meteor.

Bornstein, R. D., and A. D. Robock.
    1975. EFFECTS OF VARIABLE AND UNEQUAL TIME STEPS FOR THE ADVECTIVE
    AND DIFFUSIVE PROCESSES IN THE SIMULATION OF THE URBAN BOUNDARY LAYER.
    UCRL-75504 (preprint), Lawrence Livermore Lab.
    To be published in the Monthly Weather Review.

Bornstein, R. D., and collaborators.
    1975. THE NEW YORK UNIVERSITY URBAN AIR POLLUTION PROJECT OF 1964-1969:
    THE DATA.
    San Jose State University.
    Report No. 75-2.

Chandler, T. J.
    1967. ABSOLUTE AND RELATIVE HUMIDITIES OF TOWNS.
    Bull. Amer. Meteor. Soc., 48 (6), 394-399.

Davidson, B.
    1967. A SUMMARY OF THE NEW YORK URBAN AIR POLLUTION DYNAMICS RESEARCH
    PROGRAM.
    Air Poll. Cont. Assoc. J., 17 (3), 154-158.

Goldreich, Y.
    1974. OBSERVATIONS ON THE URBAN HUMIDITY ISLAND IN JOHANNESBURG.
    Israel J. of Earth Sciences, 23, 39-46.

Hage, K. D.
    1972. URBAN GROWTH EFFECTS ON LOW-TEMPERATURE FOG IN EDMONTON.
    Boundary Layer Meteor., 2, 334-347.

Halpern, P., C. Simon, and L. Randall.
   1971. SOURCE EMISSION AND THE VERTICALLY INTEGRATED MASS FLUX OF
   SULPHUR DIOXIDE ACROSS THE NEW YORK CITY AREA.
   J. Appl. Meteor., 10 (4), 715-724.

Ingram, W., E. Kaiser, and C. Simon.
   1965. SULFUR DIOXIDE EMISSIONS IN NEW YORK CITY.
   Unpublished tabulation, data available at Dept. of Meteor., San Jose
   State Univ.

Jacobs, A.
   1951. LARGE SCALE ASPECTS OF ENERGY TRANSFORMATIONS OVER THE OCEAN.
   Compendium of Meteorology.
   Amer. Meteor. Soc., 1057-1070.

Kopec, R. J.
   1973. DAILY SPATIAL AND SECULAR VARIATIONS OF ATMOSPHERIC HUMIDITY IN
   A SMALL CITY.
   J. Appl. Meteor., 12, 639-648.

Kuo, H. L.
   1968. THE THERMAL INTERACTION BETWEEN THE ATMOSPHERE AND THE EARTH AND
   PROPAGATION OF DIURNAL TEMPERATURE WAVES.
   J. Atmos. Sci., 25, 682-706.

Leahey, D. M., and J. P. Friend.
   1971. A MODEL FOR PREDICTING DEPTH OF THE MIXING LAYER OVER AN URBAN
   HEAT ISLAND WITH APPLICATIONS TO NEW YORK CITY.
   J. Appl. Meteor., 10, 1162-1173.

Lettau, H. H.
   1969. NOTE ON AERODYNAMIC ROUGHNESS-PARAMETER ESTIMATION ON THE BASIS
   OF ROUGHNESS-ELEMENT DESCRIPTION.
   J. Appl. Meteor., 8 (5), 828-832.

Lorenzen, A.
   1972. THE VERTICAL AND HORIZONTAL MOISTURE DISTRIBUTION IN THE NEW YORK
   CITY AREA.
   M.S. Thesis, Department of Meteorology, San Jose State University.

Oke, T. R., and C. East.
   1971. THE URBAN BOUNDARY LAYER IN MONTREAL.
   Boundary Layer Meteor., 1, 411-437.

Peterson, J. T.
   1969. THE CLIMATE OF CITIES: A SURVEY OF RECENT LITERATURE.
   U.S. Dept. HEW, PHS, NAPCA, Raleigh, N.C., 48 pp.

Shieh, L. J., B. Davidson, and J. P. Friend.
   1969. A MODEL OF DIFFUSION IN URBAN ATMOSPHERES: SO_2 IN GREATER NEW YORK.
   Presented at the Symposium on Multiple Source Urban Diffusion Models,
   Chapel Hill, North Carolina.

Tam, Y-T.
  1975. ANTHROPOGENIC MOISTURE PRODUCTION AND ITS EFFECT ON THE STRUCTURE
  OF THE BOUNDARY LAYER OVER NEW YORK CITY.
  M.S. Thesis, Dept. of Meteor., San Jose State Univ.

FIGURE CAPTIONS

Figure 1. Average vertical distribution of urban minus rural values of temperature ΔT, absolute humidity $\Delta \rho_v$, and relative humidity ΔRH for daytime periods (upper curves) and nighttime periods (lower curves).

Figure 2. Topography of study area with values given in feet above sea level. Also shown by the cross hatched area is the built up areas of New York City.

Figure 3. Isopleth analysis of anthropogenic moisture production from area sources in New York City in 10^{10} grams per year.

Figure 4. Isopleth analysis of anthropogenic moisture production from area sources in New York City in 10^{-5} gm cm^{-2} min^{-1}.

Figure 5. Fraction of annual area source emission of moisture in New York City as a function of mean daily temperature. Also shown is the ratio of the daily emission M_D to the uniform daily emission $\overline{M}_D$ (shown as the horizontal line).

Figure 6. Distribution of the perturbation specific humidity q' in gm km^{-1} after 12 hours of simulated time, i.e., at 0600 LST, for the flow over a warm, rough, wet city; values represent the deviation from those at the upwind boundary. Parameters include a geostrophic wind of 3 mps, a rural z_o of 1 metre, and an urban z_o of 3 metres.

Figure 7. Vertical variation of $\Delta q'$, the difference between the values of q' over the downwind urban edge and those at the upwind model edge, at 0600 LST for the run discussed in fig. 6.

Also shown is the vertical variation of $\theta_v'-\theta'$ at the upwind

model boundary (thin vertical line) and at the downwind

urban edge (thick curve).

Figure 8. Time variation of the horizontal wind speed at a height of

125 m. Values represent the differences in cm sec^{-1} between

the values at the upwind model boundary and those at the

downwind urban edge for the two cases discussed in the text.

The values of u_g and z_o are those given for fig. 6.

Table 1   Fuel Consumption in NYC for 1965.

Fuel Type	Uses	Annual Consumption
Bituminous coal	Space heating and firing of industrial boilers	5.4×10^6 tons
Anthracite coal	Residential space heating	0.72×10^6 tons
Distillate oil #4	Space heating of small apartment houses	1.5×10^9 gal.
Residual oil #6	Space heating of large apartment houses and operation of industrial plants and factories	2.6×10^9 gal.
Natural gas	Fuel in power plants, energy for industrial plants, space heating, and home cooking	1.67×10^{11} ft.^{3}
Gasoline	Automobiles, trucks, and buses	1.1×10^9 gal.
Diesel	Automobiles, trucks, and buses	66.6×10^6 gal.

Table 2   Composition of Natural Gas.

Paraffin Hydrocarbon	Fraction of Total Mass (%)	Water Content (%)
CH_4	93.45	186.90
C_2H_6	3.67	11.01
C_3H_8	1.78	7.12
C_4H_{10}	0.65	3.25
Others	0.45	-
	Total 100.00%	Total 208.28%

Table 3   Composition by Percent of Total Mass
of the Fuels Used in NYC.

Fuel Type	H_2 (%)	Gaseous H_2O (%)	Liquid H_2O (%)	Total H_2O (%)	H_2O Released Per Unit
Bituminous coal	5.14	46.26	2.0	48.26	0.4826 lb/lb
Anthracite coal	2.70	24.30	2.2	26.50	0.265 lb/lb
Distillate oil	11.63	104.67		104.67	7.955 lb/gal
Residual oil	11.63	104.67		104.67	8.478 lb/gal
Natural gas		208.28		208.28	0.11 lb/ft^3
Gasoline	15.00	135.00		135.00	9.315 lb/gal
Diesel	15.00	135.00		135.00	9.315 lb/gal

Table 4   Percentage of SO_2 Emitted from each Fuel Type in each Borough of NYC.

Fuel Type	Bronx	Brooklyn	Queens	Manhattan	Staten Island
Bituminous coal	1.45	8.61	32.53	37.26	70.80
Anthracite coal	2.16	1.34	0.39	1.31	1.29
Distillate oil #4	8.60	13.91	10.26	1.13	5.99
Residual oil #6	87.18	75.69	56.05	59.88	21.53
Natural gas	0.01	0.01	0.01	0.01	0.01
Gasoline	0.39	0.29	0.48	0.28	0.22
Diesel	0.21	0.15	0.28	0.13	0.16
TOTAL	100.00	100.00	100.00	100.00	100.00

Table 5

Fuel Type, Sulfur Content by Weight, and Sulfur Emission Factors for the Seven Fuel Types Used in NYC.

Fuel Type	Sulfur Content (%)	SO_2 Emission Factor
Bituminous coal	1.875	75.0 lb/ton
Anthracite coal	0.625	25.0 lb/ton
Distillate oil	0.575	85.0 lb/10^3 gal
Residual oil	2.450	390.0 lb/10^3 gal
Natural gas	4 ppm	0.6 lb/10^6 ft^3
Gasoline	0.030	5.0 lb/10^3 gal
Diesel	0.300	45.0 lb/10^3 gal

Table 6   Anthropogenic Moisture Production in NYC by Borough.

Borough	Production (10^{12} gm/year)	Percentage of Total
Queens	10.13	33
Brooklyn	8.60	28
Manhattan	7.06	23
Bronx	3.99	13
Staten Island	0.92	3
TOTAL	30.69	100

Table 7   Anthropogenic Moisture Production in NYC by Fuel Type.

Fuel Type	Production (10^{12} gm/year)	Percentage of Total
Bituminous coal	2.35	7.7
Anthracite coal	0.17	0.6
Distillate oil	5.05	16.4
Residual oil	9.93	32.3
Natural gas	8.32	27.1
Gasoline	4.59	15.0
Diesel	0.28	0.9
TOTAL	30.69	100.0

Table 8   Anthropogenic Moisture Production in NYC by Source Type.

Source Type	Production (10^{12} gm/year)	Percentage of Total
Domestic	10.91	35.5
Industrial	1.78	5.8
Government & Commercial	4.18	13.6
Power Plants	8.95	29.2
Motor Vehicle	4.87	15.9
TOTAL	30.69	100.0

Table 9   Grid locations for θ, u and v grid points, with height above the surface z indexed by j, and distance from the center of the urban area x indexed by i.

j/i	z(m)	x(km)
1	0	-30
2	12.5	-20
3	37.5	-12.5
4	62.5	- 7.5
5	87.5	- 5.0
6	125	- 2.5
7	175	0
8	225	2.5
9	275	5.0
10	325	7.5
11	375	10.0
12	450	15.0
13	600	22.5
14	850	32.5
15	1200	47.5
16	1650	67.5

Table 10 Height variation of the temperature difference due to the urban moisture excess $\Delta\theta_1$, and due to the urban heat island $\Delta\theta_2$, at a site located at the downwind urban edge.

z	$\Delta\theta_1$	$\Delta\theta_2$
(m)	(°C)	(°C)
0	0.5	5.3
12.5	0.3	4.7
37.5	0.2	2.5
67.5	0.2	2.0
87.5	0.1	1.7
125.0	0.1	1.4
175.0	0.1	1.0
225.0	0.1	0.8
275.0	0.0	0.7
325.C	0.0	0.6
375.0	0.0	0.4
450.0	0.0	0.3
600.0	0.0	0.1
850.0	0.0	0.0

ACKNOWLEDGMENTS

APPENDIX A LIST OF SYMBOLS

Variables and Constants - Roman Alphabet

$a(x,t)$	specified variation of the surface specific humidity
h	top of constant flux layer, equal to 25 m
H	top of transition layer, equal to 1900 m
i	horizontal index for horizontal wind and temperature grid
j	vertical index for horizontal wind and temperature grid
K	generalized eddy transfer coefficients in $cm^2\ sec^{-1}$
K_H	eddy transfer coefficient for heat in $cm^2\ sec^{-1}$
K_q	eddy transfer coefficient for moisture in $cm^2\ sec^{-1}$
M_A'	annual emission of moisture from a particular area source in gm per year
M_A	same as M_A', but in $gm\ cm^{-2}\ sec^{-1}$
M_D	daily emission of moisture from a particular area source grid in $gm\ cm^{-2}\ sec^{-1}$
M_i	moisture emission factor for the i-th fuel
p	atmospheric pressure in dynes cm^{-2}
p_m	constant space average of pressure in dynes cm^{-2}
p_o	variation of pressure in absence of perturbation motion in dynes cm^{-2}
p'	fluctuation of pressure due to perturbation motion in dynes cm^{-2}
P_i	percent of total SO_2 emission in a grid from use of the i-th fuel
q	specific humidity in grams of moisture per grams of moist air
q_m, q_o, q'	see pressure definitions

q_*	friction specific humidity in grams of moisture per grams of moist air
S_i	SO_2 emission factor for i-th fuel
t	time in sec
T	temperature in K
T_m, T_o, T'	see pressure definitions
u	horizontal component of wind in the x-direction in $cm\ sec^{-1}$
u_g	geostrophic wind in x-direction in $cm\ sec^{-1}$
u_*	friction velocity in $cm\ sec^{-1}$
U	total horizontal wind speed in $cm\ sec^{-1}$
v	horizontal component of wind in the y-direction in $cm\ sec^{-1}$
w	vertical component of the wind in $cm\ sec^{-1}$
x	horizontal coordination in direction of geostrophic wind in cm
y	horizontal coordinate in direction perpendicular to the geostrophic wind in cm
z	vertical coordinate for vorticity in cm
z_o	aerodynamic roughness length in cm

Variables and Constants - Greek Alphabet

Γ	dry adiabatic cooling rate, equal to 9.8 K km^{-1}
ζ	modified y-component of vorticity in sec^{-1}
θ	potential temperature in K
θ_m, θ_o, θ'	see pressure definitions
θ_v	virtual potential temperature in K
θ_v'	perturbation virtual potential temperature in K
θ_*	friction potential temperature in K
ψ	stream function in $cm^2\ sec^{-1}$
Δ	difference operator

Figure 1

Figure 2

MILES NORTH OF THE BATTERY

KILOMETERS EAST OF THE BATTERY

MILES EAST OF THE BATTERY

KILOMETERS NORTH OF THE BATTERY

Figure 3

Hornstein & Tam : 40
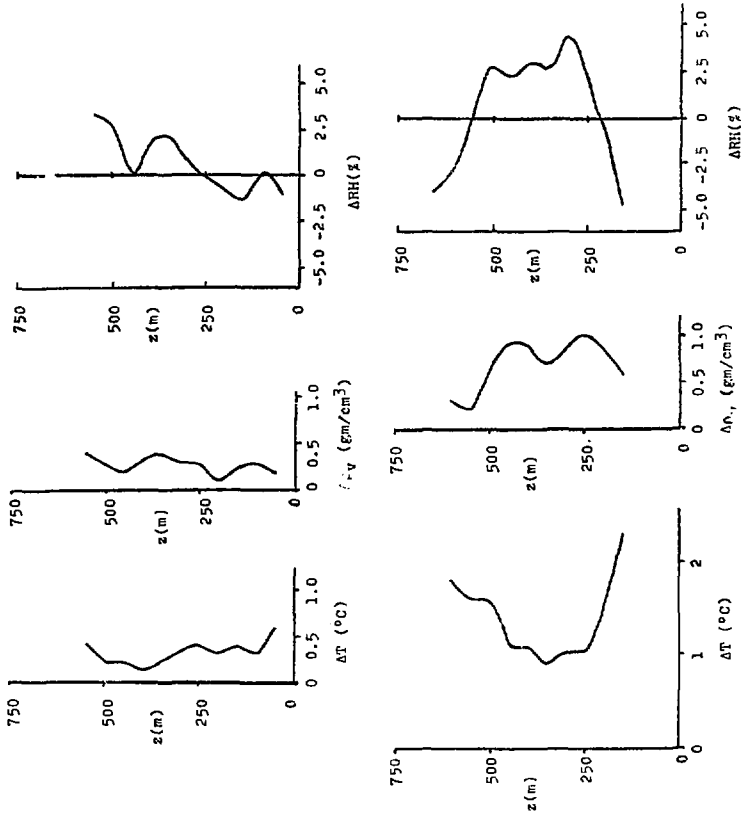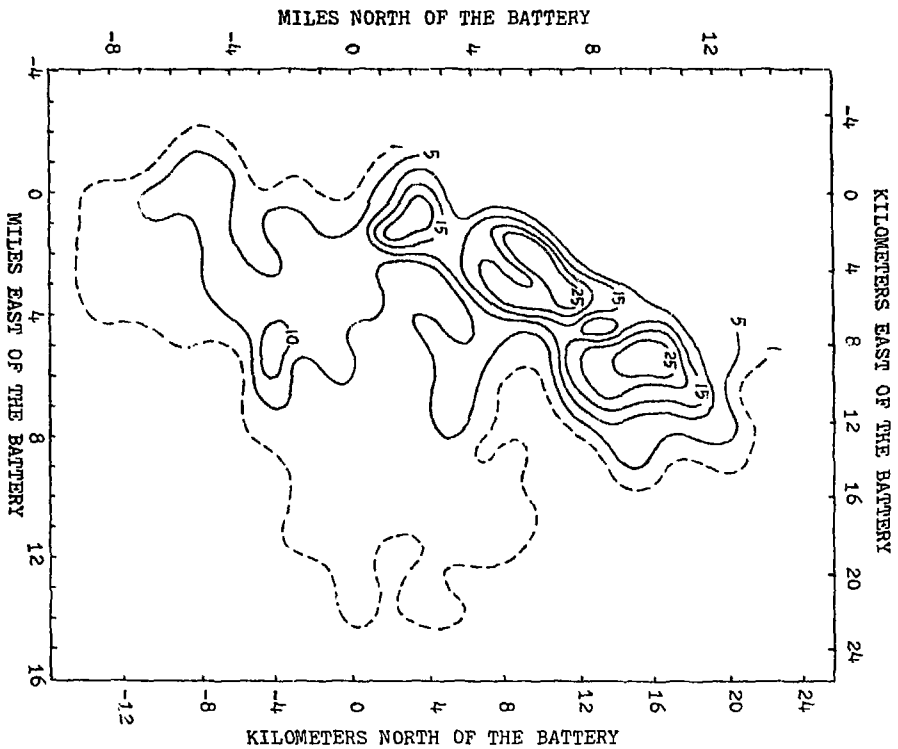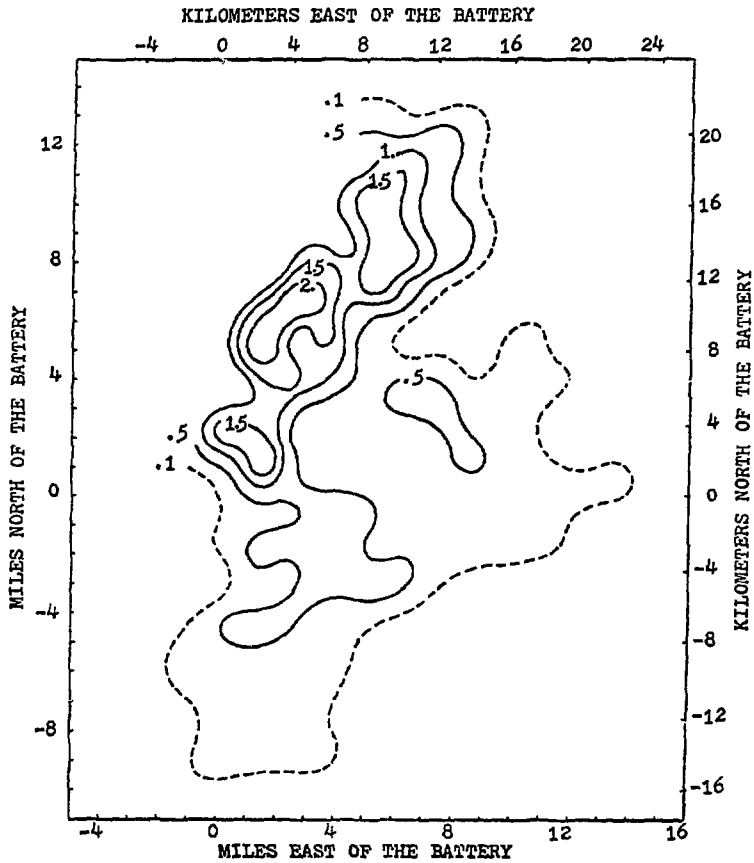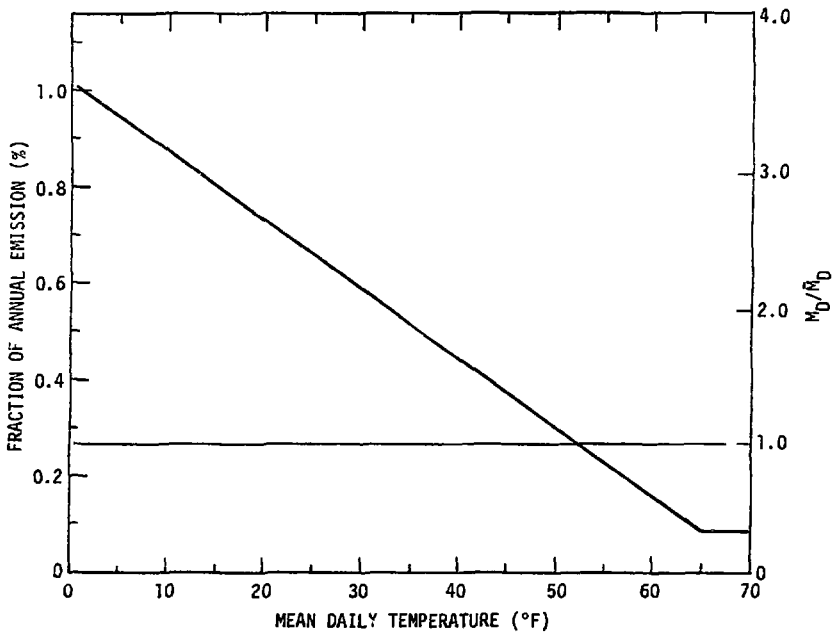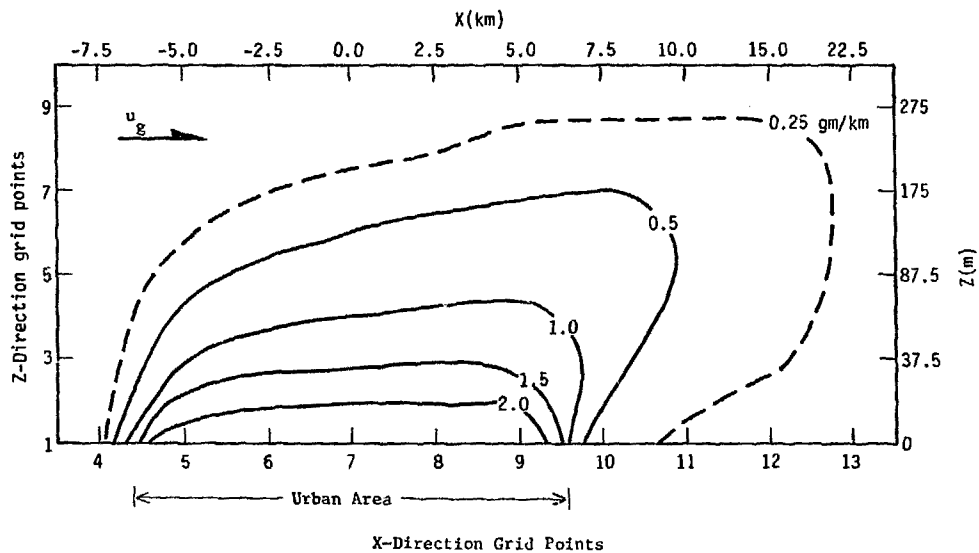
Figure 4
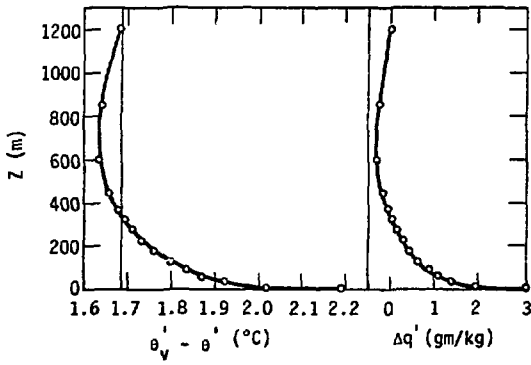
Figure 5
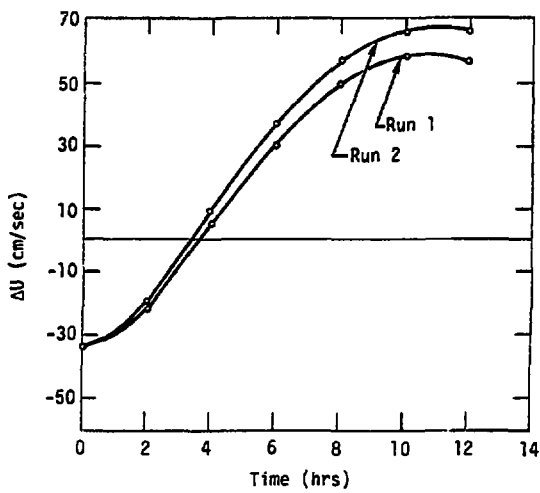
Figure 6

Figure 7

Figure 8

ABSTRACT

A heat and moisture excess over New York City is shown to exist by the analysis of helicopter soundings of temperature and wet bulb depression. The magnitude of the temporal and spatial distribution of anthropogenic moisture emissions in New York City were estimated from fuel usage data. The URBMET urban boundary layer model was used to evaluate the effects on the dynamics of the urban boundary layer resulting from the observed urban moisture excess. Work is currently in progress which seeks to determine the fraction of the observed moisture excess over New York that is due to anthropogenic sources.